

Research Paper ■

## Enhanced Electrostatic AChE Activity of Abnormally Hydrophobic Environment in Alzheimer's Plaques

**Rakesh Sharma**

**Abstract.** Computational techniques based on Brownian dynamics simulation speculate the electrostatic and kinetic properties of Acetylcholinesterase (AChE) in the range of dielectric constant values 60-78. Typically the enzyme specific to Alzheimer's Disease has specificity constant ( $k_{cat}/K_m$ ) of AChE at both dielectrics constants. AChE is distributed heterogeneously within the senile plaques and neurofibrillary tangles (NFTs) of Alzheimer's Disease (AD). The role of decreased brain AChE has been highlighted as responsible for specific Magnetic Resonance Spectroscopic pattern profiles in AD. These findings strengthen the suggestion that the altered AChE in AD may be associated with specific MR spectral peak patterns. This phenomenon may account for the reduced levels of the ACh neurotransmitter in the cerebral tissue of Alzheimer's disease (AD) patients. These results can be useful in clinical trials on AD lesions.

■ **Infor Med Slov:** 2008; 13(1): 9-14

---

Author's institution: Department of Chemical & Biomedical Engineering, FAMU-FSU College of Engineering, Tallahassee, Florida, USA.

Contact person: Rakesh Sharma, 901 West Jefferson Street, Jeffwood B-7, Tallahassee, FL 32304, USA. email: rs2010@columbia.edu.

## Introduction

### Alzheimer's disease

Alzheimer's disease (AD) has manifestations of senile plaques and neurofibrillary tangles (NFTs) in the cerebral cortex involving hippocampus of Alzheimer's brains. Many studies have shown that the levels of the reduced ACh neurotransmitter in AD brain had been curiosity in recent past. In this direction, promising success is claimed in drug therapeutic trials based on AChE inhibitors. In AD presumably five neurological cell groups are commonly seen around the cortex rich with AD lesions associated with the low AChE enzyme. Other important problem of AD therapeutics was solved by use of higher concentrations of AChE inhibitor, such as tacrine, physostigmine, and BW284C51, to inhibit AChE within AD lesions. Simultaneously, elevated levels of the ACh substrate also inhibit AChE activity. Serotonin, 5-hydroxytryptophan, carboxypeptidase inhibitor, and bacitracin have proven good choice to effectively inhibit cholinesterase activity within plaques and tangles, but fail to alter the AChE activity in normal tissue at standard physiological conditions.

This paper offers electrostatic explanation of lowered AChE catalytic activity in AD brain tissue over normal tissue with possibility of the protein-rich deposits associated with the onset of AD. The high concentration of protein-rich deposits in plaques and NFTs such as alpha amyloid protein ( $\alpha$ AP), heparan and dermatan sulfate proteoglycans, serum amyloid P component, complement factors, and protein kinase C, has been an active research topic together with the increased hydrophobicity of AChE in AD lesions and abnormally reduced dielectric constant. AChE catalysis has been explained as electrostatic screening mechanism where altered dielectric conditions correspond to  $\beta$ AP deposition. Possibly, dielectric constant shift in AD tissue also allows Coulombic interactions to permeate longer distances resulting in enhanced enzymatic activity and simultaneously decreased ACh levels. MR

spectral pattern of enhanced choline also supports association with decreased ACh levels in AD.

### Acetylcholinesterase

The acetylcholinesterase enzyme (AChE) has 537 amino acid long polypeptide in the postsynaptic neural membranes of central nervous system and neuromuscular junctions by a glycosylphosphatidylinositol linkage. AChE catalyzes the hydrolysis of the acetylcholine (ACh) substrate neurotransmitter at cholinergic synapses. AChE hydrolysis results in the termination of impulse transmission.

The determination of the three-dimensional structure of AChE dimer enzyme comprises 12-stranded mixed  $\beta$ -sheet surrounded by 14  $\alpha$ -helices. These subunits assemble through disulfide linkage and hydrophobic interactions. The enzyme structure shows structural characteristic of AChE as a deep ( $\sim 20\text{\AA}$ ), narrow active site making enzyme's catalytic site Ser<sup>200</sup>, His<sup>440</sup>, and Glu<sup>327</sup> at its base. The walls of this entity are lined with 14 highly conserved aromatic amino acids of active site. Positively charged ACh substrate towards the active site causes low-affinity cation- $\pi$  interactions. Further, amino acid charge distribution over AChE creates an electric field around the enzyme contributing to its enzymatic activity (electrostatic steering mechanism) involving its substrate, ACh. Authors determined that the negative field drives the positively-charged ACh substrate molecule toward the entrance of its active site moiety and increases the catalytic rate of ACh.

## Theory

### Electrostatics

If partial atomic charges are assigned according to the OPLS parameter set at neutral pH, generating a net charge of  $-10e$ ,<sup>1</sup> Coulombic electrostatic forces between the AChE monomer and ACh may be calculated by centering the enzyme in a  $64^3$  grid

lattice with 4 Å spacing and using the following equation to compute the electrostatic force at each point on the grid:

$$F(r) = \frac{e^2}{\epsilon} \sum_{i=1}^N \frac{q_i d_i}{d_i^3} (1 + \kappa d_i) e^{(-\kappa d_i)} \quad (1)$$

where  $e$  is the charge on an electron,  $\epsilon$  is the dielectric constant of the system,  $N$  is the number of atoms in the enzyme,  $q_i$  is the charge of the  $i^{\text{th}}$  enzyme atom,  $d_i$  is the distance between the  $i^{\text{th}}$  enzyme atom and the grid point, and  $\kappa$  is the Debye-Hückel ion screening parameter which approximately accounts for the perturbation of solvent ions on charge-charge interactions between the enzyme and its substrate. This ion screening parameter is defined as

$$\kappa = \sqrt{\frac{2N_A \rho e^2 I}{\epsilon_0 \epsilon k_B T}} \quad (2)$$

where  $N_A$  is Avagadro's number,  $\rho$  is the density of the solvent,  $I$  is the ionic strength of the solvent,  $\epsilon_0$  is the permittivity of vacuum,  $k_B$  is Boltzmann's constant, and  $T$  is the absolute temperature of the system.

### Brownian dynamics

Diffusion-controlled rate constants were obtained by simulating the reaction of AChE with an ensemble of ACh substrate molecules using the theory of Brownian dynamics. This was accomplished by dividing the space around AChE with a spherical surface of radius  $b$  and another with a larger radius  $q$ , such that all electrostatic interactions beyond  $b$  were centrosymmetric and substrate flux was isotropic.

The diffusional trajectory of an ACh molecule was calculated by randomly placing it on the  $b$  sphere and using the following Ermak-McCammon algorithm to compute subsequent motion:

$$r = r^o + \frac{D_{rel} F(r) \Delta t}{k_B T} + S \quad (3)$$

where  $r^o$  and  $r$  are the locations of ACh before and after a trajectory step is taken, respectively,  $D_{rel}$  is the relative diffusion constant,  $\Delta t$  is the length of a trajectory time step, and  $S$  represents a stochastic force due to collisions with solvent molecules having the statistical properties of a Gaussian distribution with zero mean and variance equal to  $2D_{rel}\delta_{ij}\Delta t$ , where  $\delta_{ij}$  is the Kronecker delta.<sup>2</sup> The electrostatic force on the substrate was calculated by interpolating the pre-calculated force values of the nearest grid points on the lattice by using a three-dimensional Taylor's expansion and solving the derivatives with the method of finite differences.<sup>3</sup> A trajectory terminated once the substrate diffused to within a certain distance of the enzyme's active site or beyond the established  $q$  sphere. Numerous trajectories were computed to yield a reaction probability of  $\beta$ , which was utilized in the following expression to solve for the diffusion-controlled rate constant:

$$k = k_D(b)\beta[1 - (1 - \beta)\Omega]^{-1} \quad (4)$$

where  $\Omega$  is the probability of a substrate diffusing past the  $q$  sphere and then returning and  $k_D(b)$  is the steady-state rate constant at which the ACh molecules penetrate the  $b$  sphere.<sup>4</sup> The following expression has been derived to describe this term:

$$k_D(b) = 4\pi D_{rel} \left( \int_b^{\infty} \frac{e^{\frac{U}{k_B T}}}{r^2} dr \right)^{-1} \quad (5)$$

where  $U$  is the intermolecular potential of mean force and  $r$  is equivalent to the radius of the constructed  $b$  sphere.<sup>5</sup>

### Model system

The use of the *Torpedo californica* AChE crystal structure for studying the pathogenesis of AD is supported by the primary sequence homology of

the electric eel and human enzymes.<sup>6</sup> Molecular modeling was used to determine that the hydrodynamic radius of the AChE monomer and ACh were  $\sim 30$  Å and 4.23 Å, respectively. However, to approximate the active site wall fluctuations of the narrow gorge of AChE, the substrate was modeled as a positively charged sphere with a radius of 2 Å.<sup>7</sup> To verify the dependence of the rate constant on the substrate radius parameter, test simulations were performed at various radii values. All non-hydrogen protein atoms were modeled as spheres with radii of 1.5 Å.<sup>3</sup> In addition, the  $b$  and  $q$  spherical radii were assigned distances of 128 Å and 295 Å, respectively. Reaction criteria were satisfied when the substrate sphere diffused within 15 Å of the OG atom of the Ser<sup>200</sup> catalytic residue. A variable time step algorithm was used with  $\Delta t$  values ranging from 1.25 fs to 800 ps as the substrate approached the outer  $q$  sphere.

Simulations were performed using 8000 trajectories at a temperature of 300 K, an ionic strength of 5 mM, a solvent density of 996.5 kg/m<sup>3</sup>, and dielectrics of 78 and 60. The Brownian dynamics program written for this work was compiled for use on a personal desktop computer, which presented operating system memory allocation problems. This program circumvents this limitation by utilizing a virtual addressing method.<sup>8</sup> All calculations were performed on a Packard Bell personal computer equipped with an Intel Pentium processor.

## Results and discussion

### Ionic strength

Computed rate constants of *Torpedo californica* AChE at various ionic strengths are given in Table 1. These values are compared with experimental bimolecular association constants ( $k_f$ ) and enzymatic specificity constants ( $k_{cat}/K_m$ ) of a related *Electrophorus electricus* AChE enzyme.<sup>9</sup> Since the association constant considers the binding event of the reaction and the specificity

constant describes both binding and subsequent catalytic turnover,  $k_f$  is the theoretical maximum value for the calculated diffusion-controlled rate constant, while  $k_{cat}/K_m$  sets the lower limit on these second-order reactions. As seen in Figure 1, the calculated rate constants found in this work lie between these two extremes throughout the range of ionic strengths tested. This provides encouraging support for the ionic screening approximations used in this work. Furthermore, the decrease in the rate of AChE catalysis with increasing ionic strength provides strong evidence that an electrostatic steering mechanism plays a role in AChE kinetics. The similarity in the negative slope observed for both association and specificity constants indicates that the ligand binding step of the reaction is dependent upon solvent salt concentration.

**Table 1** Effect of Dielectric on Activity of wt AChE. 8000 trajectories were simulated at 300 K, an ionic strength of 5 mM, a solvent density of 996.5 kg/m<sup>3</sup>, and a pH of 7.0.

Dielectric	Rate constant (M <sup>-1</sup> s <sup>-1</sup> )	Standard error
78	$1.3 \times 10^9$	$0.267 \times 10^9$
60	$4.7 \times 10^9$	$0.615 \times 10^9$

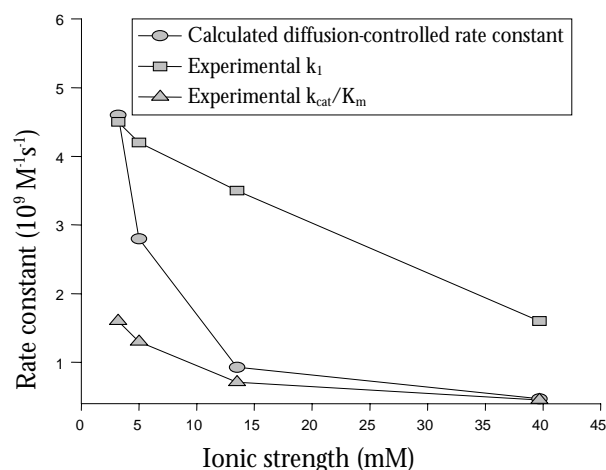


**Figure 1** Experimental and calculated rate constants versus ionic strength. Calculations for preliminary ionic strength study used 1000 trajectories at a temperature of 298 K, a dielectric of 78, a solvent density of 997.0 kg/m<sup>3</sup>, and a pH of 7.0.

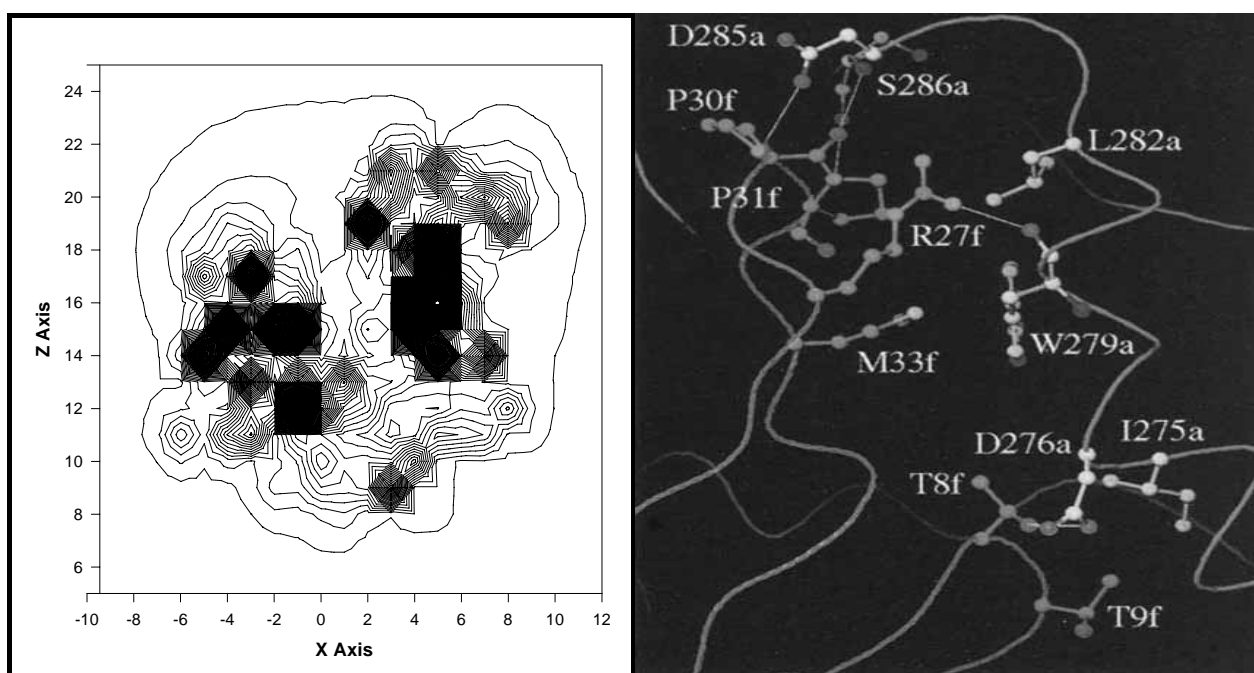


**Figure 2** Left: Electric field of AChE at an aqueous dielectric ( $\epsilon=78$ ). Active site gorge extends between  $z=14$  and  $z=20$ . Electric field contours =  $5 \times 10^{-12}$  N, x-axis represents the location of the catalytic Ser<sup>200</sup> residue and each grid unit is 4 Å. Right: Interface with interacting residues shown as ball-and-stick models of AChE covering AChE residues 68-90 and AChE residues 271-289 as active (a) and fused (f).

### Substrate radius

To demonstrate the limited accessibility of this enzyme's active site structure, simulations were performed using various substrate radii (Figure 1). It is reasonable to predict increased rate constant values with a reduced substrate radius since the probability of a smaller substrate penetrating the active site gorge and reacting with AChE is higher. The results shown in Figure 2 show this expected trend. These computed rate constants also compare well with the approximated specificity constant of  $4.2 \times 10^9 \text{ M}^{-1}\text{s}^{-1}$  for *Electrophorus electricus* AChE at zero ionic strength.<sup>9</sup>

It has been hypothesized that the active site gorge of AChE undergoes conformational fluctuations to allow substrate entry.<sup>7</sup> Further simulation calculations in this work have used a smaller substrate radius (2 Å) than the actual hydrodynamic radius of ACh (4.23 Å) to approximately account for this protein flexibility.

### Reduced dielectric in plaques and NFTs

Simulations of the AChE-ACh reaction at both aqueous ( $\epsilon=78$ ) and hydrophobic ( $\epsilon=60$ ) conditions demonstrate the substantial effect of the AChE environment on its catalytic activity. The results of this study in Table 1 reveal that the abnormally low dielectric medium of the enzyme increases its catalytic rate by a factor of 3.6. These results are experimentally supported by Nolte et al.,<sup>9</sup> who found a rate constant of  $1.6 \times 10^9 \text{ M}^{-1}\text{s}^{-1}$  for *Electrophorus electricus* AChE under similar conditions.

These findings are complemented by the visualization of an intensified electric field near the entrance of the AChE active site gorge in the reduced dielectric environment. This observation can be made by comparing the electric field contours around the perimeter of AChE at dielectrics of 78 and 60 (Figure 2). These contour plots illustrate an electrostatic gradient emerging from the gorge entrance and extending along the

enzyme's surface. This effectively enlarges the active site target area, resulting in increased enzyme-substrate association. These electric field calculations along the protein's surface are consistent with the results of Antosiewicz et al.,<sup>7</sup> who have suggested that electrostatic steering is limited to operation near the surface of the enzyme. The contour plots found in this work also offer a plausible explanation for the catalytic rate constant enhancement at lower dielectrics and further suggest that electrostatic attraction is an important component of the AChE mechanism and ultimately its physiological role in the human nervous system.

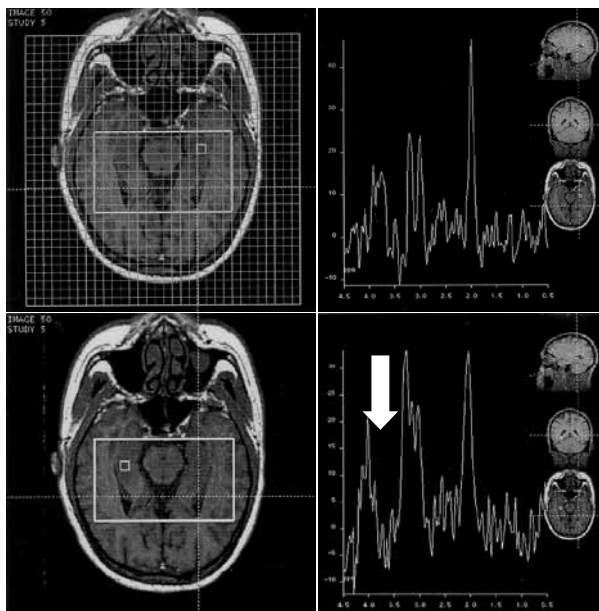


**Figure 3** A comparison is shown between normal hippocampus MR spectroscopy Choline peak (normal brain peaks) and Alzheimer's Disease abnormal high Choline peak shown with an arrow (in panel at the bottom) due to reduced AChE.

The reduced AChE enzyme activity is also supported by high and localized Choline MR spectroscopy in AD brain as shown in Figure 3. In our previous data, the single voxel point resolved MR spectroscopy suggested strongly the enhanced choline peaks at scan parameters TE = 135 ms, TR= 5000 ms, pointing out the active role of AChE in active plaques and neurofibrillary tangles. However, other dielectric and physical

factors also play role in development of AD lesions and plaques.

## Conclusions

Abnormal Magnetic Resonance spectral peak patterns are associated with low AChE in AD, which is due to enhanced increasing ACh breakdown and surrounding electrostatic field of this enzyme.

## References

1. Jorgensen WL, Tirado-Rives J: The OPLS Potential Functions for Proteins. Energy. Minimizations for Crystals of Cyclic Peptides and Crambin. *J Am Chem Soc* 1988; 110(6):1657-1666.
2. Ermak D, McCammon J: Brownian Dynamics with Hydrodynamic Interactions. *J Chem Phys* 1978; 69: 1352-1360.
3. Allison SA, Bacquet RJ, McCammon JA: Simulation of the Diffusion-Controlled Reaction Between Superoxide and Superoxide Dismutase II: Detailed Models. *Biopolymers* 1988; 27: 251-269.
4. Northrup SH, Allison SA, McCammon JA: Brownian Dynamics Simulation of Diffusion-Influenced Bimolecular Reactions. *J Chem Phys* 1984; 80(4): 1517-1524.
5. Northrup S, Hynes JT: Short range caging effects for the reactions in solutions, part I: reaction constants and short range caging picture; part II: escape probability and time dependent reactivity. *J Chem Phys* 1979; 71: 871-893.
6. Cygler M, Schrag JD, Sussman JL, et al.: Relationship between sequence conservation and three-dimensional structure in a large family of esterases, lipases, and related proteins. *Protein Science* 1993; 2, 3: 366-382.
7. Antosiewicz J, McCammon J, Wlodek S, et al.: Simulation of Charge-Mutant Acetylcholinesterases. *Biochemistry* 1995; 34: 4211-4219.
8. Yu Y, Marut C: *Assembly Language Programming and Organisation of IBM PC*. 1992:McGrawhill Inc.
9. Nolte H, Rosenberry T, Neumann E: Effective Charge on Acetylcholinesterase Active Sites Determined from the Ionic Strength Dependence of Association Rate Constants with Cationic Ligands. *Biochemistry* 1980; 19: 3705-3711.